Sādhanā Vol. 31, Part 4, August 2006, pp. 445–461. © Printed in India

Solution of Fokker–Planck equation by finite element and finite difference methods for nonlinear systems

PANKAJ KUMAR and S NARAYANAN

Department of Mechanical Engineering, Indian Institute of Technology – Madras, Chennai 600 036, India
e-mail: narayans@iitm.ac.in

Abstract. The response of a structural system to white noise excitation (delta-correlated) constitutes a Markov vector process whose transitional probability density function (TPDF) is governed by both the forward Fokker–Planck and backward Kolmogorov equations. Numerical solution of these equations by finite element and finite difference methods for dynamical systems of engineering interest has been hindered by the problem of dimensionality. In this paper numerical solution of the stationary and transient form of the Fokker–Planck (FP) equation corresponding to two state nonlinear systems is obtained by standard sequential finite element method (FEM) using C^0 shape function and Crank–Nicholson time integration scheme. The method is applied to Van-der-Pol and Duffing oscillators providing good agreement between results obtained by it and exact results. An extension of the finite difference discretization scheme developed by Spencer, Bergman and Wojtkiewicz is also presented. This paper presents an extension of the finite difference method for the solution of FP equation up to four dimensions. The difficulties associated in extending these methods to higher dimensional systems are discussed.

Keywords. Fokker–Planck equation; finite element method; finite difference method; random vibration; nonlinear stochastic dynamics.

1. Introduction

Response of nonlinear systems to random excitation has been the topic of investigation for a number of years by many researchers. It is well known that the response of a nonlinear dynamical system to random excitation having delta-correlation constitutes a Markov vector process whose transition probability density function is governed by an appropriate Fokker–Planck (FP) equation. To compute the response statistics the FP equation has to be solved under certain boundary and singularity conditions. Unfortunately, for systems of engineering interest, no closed form solution of FP equation is available. Exact solutions for the FP equation are available only for a few linear system (Wang & Uhlenbeck 1945; Lin 1967; Soong 1994), scalar system (Caughey & Dienes 1962) and for some Multi-dimensional conservative

This paper is dedicated to Prof R N Iyengar of the Indian Institute of Science on the occasion of his formal retirement.

systems (Caughey 1971; Wen 1976; Kunert 1991). The difficulty of solving the FP equation has led to a number of approximate methods such as the equivalent linearization method (Roberts & Spanos 1990), perturbation method (Crandall 1963), stochastic averaging method (Khasminskill 1996), and various closure methods (Wojtkiewicz *et al* 1996; Wu & Lin 1984). Monte-Carlo simulation (MCS) techniques can be applied in general to a large class of nonlinear systems subjected to random excitation and its accuracy is, in principle, independent of the type of nonlinearity. However, the method requires large computational resources, especially for computing the tail probabilities of a distribution required in reliability studies (Johnson *et al* 1997; Schueller *et al* 1993).

In recent years, the shift has been towards numerical methods of solution of the FP equation. The numerical methods based on the Markov vector assumptions have been proposed for the solution of the FP equation such as the finite element method by Langley (1985), Langtangeh (1991), Spencer & Bergman (1993), Wojtkiewicz *et al* (1994) and Johnson *et al* (1997), finite difference method by Johnson *et al* (1997) and Wojtkiewich *et al* (1994b), path integral method by Naess & Johnson (1992) and the cell-mapping method by Sun & Hsu (1990, 1998). All the numerical solution techniques developed for the FP equation so far are confined to a phase-space vector dimension of order < 4. The numerical methods suffer from difficulties of treating higher dimensional problems, requirement of large computer memory and loss of accuracy of the probability density function (PDF) in the tail regions.

Many of the methods mentioned above have been restricted to the study of the stationary solution of the FP equation. The transient solution however is also of importance, especially in estimating the first passage failure probability, where failure or first excursion from the safe domain may occur long before stationarity is achieved.

This paper presents the finite element method and higher order finite difference method for transient and stationary solution of the FP equation for some nonlinear systems subjected to parametric and external stochastic excitation. This paper also presents a higher order finite difference scheme to solve the FP equation associated with a nonlinear system with four-dimensional state vectors. The difficulties associated in extending the method to still further higher dimensions are discussed.

2. Basic problem formulation

Many stochastic systems may be modelled with n-dimensional vector Itô stochastic differential equations (SDE) of the form,

$$\mathrm{d}\mathbf{X}/\mathrm{d}t = \mathbf{m}(\mathbf{X}) + \mathbf{G}(\mathbf{X})\mathbf{W}(t), \tag{1}$$

where $\mathbf{X}$ is an R^n valued stochastic process. $\mathbf{m(X)}$ and $\mathbf{G(X)}$ are the drift vector and the diffusion matrix respectively. $\mathbf{W}(t)$ is an m-dimensional vector of uncorrelated white noise. The vector of white noise is fully defined by the first and second moments of its components given by,

$$\begin{aligned} &E[W_i(t)] = E[W_j(t)] = 0,\ E[W_i(t_1)W_j(t_2)] = 2\mathbf{D}_i\delta(\tau), \\ &E[W_i(t)W_j(t)] = 0 \text{ and } \tau = t_2 - t_1, \end{aligned} \tag{2}$$

where $\mathbf{D}_i$ is the spectral density of the ith excitation and $\delta(\tau)$ is the Dirac delta function, $E[]$ denotes the expectation operation. The aforementioned system forms a Markov vector process in R^n, the behaviour of which is completely determined by the transition probability density

function $p(\mathbf{X}, t|\mathbf{X}_0)$. The transition probability density function is proportional to the probability of being in a differential element $(\mathbf{X}, \mathbf{X}+\mathrm{d}\mathbf{X})$ of the phase plane at time t, having started at $\mathbf{X}_0$ at time zero and satisfies both the forward (FP) and the backward Kolmogorov equations.

The FP equation associated with equation (1) can be derived from the Itô form.

$$\mathrm{d}\mathbf{X}(t) = \mathbf{m}(\mathbf{X})\mathrm{d}t + \mathbf{G}(\mathbf{X})\mathrm{d}\mathbf{B}(t), \tag{3}$$

where $\mathbf{B}(t)$ is a vector Wiener process and $\mathbf{m}(\mathbf{X})$ is the Wong & Zakai (1965) corrected drift vector.

The FP equation for the system is given by (Risken 1989),

$$\frac{\partial p}{\partial t} = -\sum_{i=1}^{n} \frac{\partial \left[m_i(X)p\right]}{\partial x_i} + \sum_{i=1}^{n}\sum_{j=1}^{n} \frac{\partial^2 \left[h_{ij}(X)p\right]}{\partial x_i \partial x_j}, \tag{4}$$

where h_{ij} is the ijth element of the matrix $\mathbf{H}(\mathbf{x}) = \mathbf{G}(\mathbf{X})\mathbf{D}\mathbf{G}^T(\mathbf{X})$ and $p = p(\mathbf{X}, t|\mathbf{X}_0)$ is the transition probability density function of $\mathbf{X}(t)$ with normalization condition

$$\int_{R^n} p(\mathbf{X}, t|\mathbf{X}_0)\mathrm{d}\mathbf{X} = 1 \tag{5}$$

subjected to the initial condition

$$\lim_{t\to 0} p(\mathbf{X}, t|\mathbf{X}_0) = \delta(\mathbf{X} - \mathbf{X}_0). \tag{6}$$

Additionally a zero flux condition is imposed at infinity, given by

$$p(\mathbf{X}_i, t) \to 0 \text{ as } [\mathbf{X}_i] \to \pm\infty, i = 1, 2, \ldots, n. \tag{7}$$

3. Finite element approach

The first step in the numerical solution of an initial and boundary value problem is the spatial discretization by which the transformation of a system of partial differential equations to a system of ordinary differential equations is achieved. The weighted residual statement for the problem given by (4) is integrated by parts to produce the weak form of the equations and the shape functions are chosen, which are defined for a finite region of the domain only. In this way, a set of linear equations is constructed in which the unknowns are the values of the joint probability density function at a number of nodes in the domain. These equations are then solved by standard matrix methods.

The solution to (4) using a standard Bubnov–Galerkin finite element formulation is as follows. The relevant portion Ω of the phase space is divided into $M(56)$ elements, each with $m(72)$ nodes spanning the domain Ωe as in figure 1 for a two-dimensional system.

The probability density function (PDF) within the eth element is interpolated according to the scheme.

$$\hat{p}(\mathbf{X}, t|\mathbf{X}_0) = \sum_{s=1}^{m} N_s(\mathbf{X}) p_s^e(\mathbf{X}, t|\mathbf{X}_0), \mathbf{X} \in \Omega, \tag{8}$$

where $N_s(\mathbf{X}), s = 1, 2 \ldots, m$, are the element shape functions, m denotes the number of nodes in a single element and the p_s^e are the values of the probability density function at the nodes.

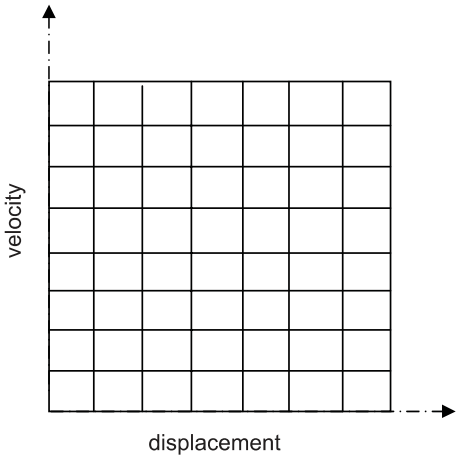

Figure 1. Finite element mesh used for two-dimensional system.

As (4) in the present form contains second-order terms, the shape functions chosen for PDF must be at least C^1 continuous. This is inconvenient as for an ideal finite element formulation for calculating PDF at any point using linear interpolation between the nodes, functions which have only C^0 continuity are required. This problem can be overcome by integrating (4) by parts to produce the weak form of the equation in which C^0 continuity is sufficient.

Converting (4) into the weak form and choosing the shape functions such that the residuals are orthogonal to the shape functions gives,

$$\sum_{e=1}^{M}\int_{\Omega e}\left[\frac{\partial \hat{p}}{\partial t}N_r(\mathbf{X})\mathrm{d}\mathbf{X}+\sum_{i=1}^{n}m_i(\mathbf{X})\hat{p}(\mathbf{X})\frac{\partial}{\partial x_i}[N_r(X)]\mathrm{d}\mathbf{X}\right.$$
$$\left.-\sum_{i=1}^{n}\sum_{j=1}^{n}\frac{\partial}{\partial x_i}\left[N_r(X)\frac{\partial}{\partial x_j}[h_{ij}(X)\hat{p}(X)\right]\mathrm{d}\mathbf{X}\right]=0 \tag{9}$$

Substituting (8) in (9) and expanding gives,

$$\sum_{e=1}^{M}\sum_{s=1}^{m}[\dot{p}_s^e(\mathbf{X},t|\mathbf{X}_0)C_{rs}^e+p_s^e(\mathbf{X},t|\mathbf{X}_0)K_{rs}^e]=0, \tag{10}$$

where

$$C_{rs}^e=\int_{\Omega e}N_r(\mathbf{X})N_s(\mathbf{X})\mathrm{d}\mathbf{X}, \tag{11}$$

and

$$K_{rs}^e=\int_{\Omega e}\left[\sum_{i=1}^{n}m_i(\mathbf{X})N_s\frac{\partial}{\partial x_i}[N_r]\mathrm{d}\mathbf{X}-\sum_{i=1}^{n}\sum_{j=1}^{n}\frac{\partial}{\partial x_i}[N_r]\frac{\partial}{\partial x_j}[h_{ij}N_s]\mathrm{d}\mathbf{X}\right]. \tag{12}$$

Globally assembling all elements, a set of n equations can be constructed, which in matrix form is given by

$$\boldsymbol{C}\dot{\boldsymbol{p}}+\boldsymbol{K}\boldsymbol{p}=0, \tag{13}$$

with initial condition $\boldsymbol{p}(0) = \boldsymbol{p}$ where $\boldsymbol{p}$ is a vector containing the values of the joint probability density function at the nodal points.

Having addressed the issue of spatial discretization, the next step is temporal discretization, that is converting the system of first-order ODE's to a set of linear algebraic equations. So this equation is further discretized in time using the θ method giving the recurrence relation,

$$[\boldsymbol{C} - \Delta t(1-\theta)\boldsymbol{K}]\boldsymbol{p}(t+\Delta t) = [\boldsymbol{C} + \Delta t\theta\boldsymbol{K}]\boldsymbol{p}(t), \tag{14}$$

where $0 \leq \theta \leq 1$ and Δt is the time step. The Crank–Nicholson scheme is applied with $\theta = 0{\cdot}5$ for stability which gives

$$\left[\boldsymbol{C} - \frac{\Delta t}{2}\boldsymbol{K}\right]\boldsymbol{p}(t+\Delta t) = \left[\boldsymbol{C} + \frac{\Delta t}{2}\boldsymbol{K}\right]\boldsymbol{p}(t). \tag{15}$$

For the stationary solution of the FP equation the matrix equation (13) becomes a system of n homogeneous linear equations,

$$\boldsymbol{K}\boldsymbol{p} = 0, \tag{16}$$

where n is the number of nodal points in the computational mesh, $\boldsymbol{K} \in R^n x R^n$ and $\boldsymbol{p} \in R^n$. This system admits both a trivial solution $\boldsymbol{p} = \boldsymbol{0}$ and a nontrivial solution through enforcement of the normalization condition as given in (5).

The nontrivial solution is obtained by first fixing the PDF $\boldsymbol{p}^{\boldsymbol{C}}$ at the node corresponding to the origin as unity. This degree of freedom becomes constrained and is treated as an additional boundary condition. The solution of (16) is reduced to the solution of a system of $(n-1)$ non-homogeneous equations given by,

$$\boldsymbol{K}^r\boldsymbol{p}^r = -\boldsymbol{f}^r, \tag{17}$$

where $\boldsymbol{K}^r \in R^{n-1}x R^{n-1}$, $\boldsymbol{p}^r \in R^{n-1}$ and $\boldsymbol{f}^r \in R^{n-1}$. The reduced matrix $\boldsymbol{K}^r$ is obtained by removing the cth row and column from the original matrix $\boldsymbol{K}$ and reduced nodal density vector $\boldsymbol{p}^r$ is obtained from the original nodal density vector $\boldsymbol{p}$ by removing the cth component. The vector $\boldsymbol{f}^r$ is the cth column of $\boldsymbol{K}$ after removing the cth component. The solution of the stationary FP equation is obtained by enforcing the normalization condition given in (5).

4. Two-dimensional stationary system

To illustrate the performance and abilities of the FEM-based numerical procedure two specific cases of the Van-der-Pol oscillator driven by Gaussian white noise are considered as examples.

$$\ddot{X} + 2\xi[X(t)^2 - 1]\dot{X}(t) + X(t) = W(t), \tag{18}$$

with

$$E[W(t)] = 0,\ E[W(t)W(t+\tau)] = 2\mathbf{D}\delta(\tau). \tag{19}$$

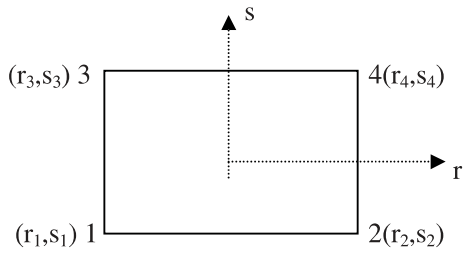

Figure 2. Four-node bilinear finite element.

For the first case $\xi = 0{\cdot}1$ and $\mathbf{D} = 0{\cdot}1$ which represents an intermediate case between linear and distinctly nonlinear behaviour while for the second example $\xi = 1{\cdot}0$ and $\mathbf{D} = 0{\cdot}1$ in which nonlinear behaviour is strongly dominant.

The grid size is taken as $[-5, 5] \times [-5, 5]$ which is divided into 100 elements per dimension each having 2^n-nodes where n is the dimensionality. In this case $n = 2$. We can use any C^0 continuity shape functions like the isoparametric or Lagrangian shape functions. Here, for the two-dimensional problem, the shape functions chosen are the Lagrangian interpolation shape functions for bilinear 4-node element (figure 2) given by,

$$N_1 = \frac{r - r_2}{r_1 - r_2}.\frac{s - s_4}{s_1 - s_4},\ N_2 = \frac{r - r_1}{r_2 - r_1}.\frac{s - s_3}{s_2 - s_3},$$
$$N_3 = \frac{r - r_4}{r_3 - r_4}.\frac{s - s_2}{s_3 - s_2},\ N_4 = \frac{r - r_3}{r_4 - r_3}.\frac{s - s_1}{s_4 - s_1}, \tag{20}$$

The results for stationary distribution for the first case are presented in the three-dimensional view of the joint PDF in figure 3a while figure 3b gives its contour plot.

For the second case the stationary joint PDF, contour plot and marginal PDF of displacement obtained by this method are shown in figures 4a, b and c respectively. Agreement between the FEM results and the analytical results is very good even for very low probability levels, which would be adequate for most extreme value analysis. In figure 4c the analytical solution is given by the full line and the FE solutions are given by the symbol •.

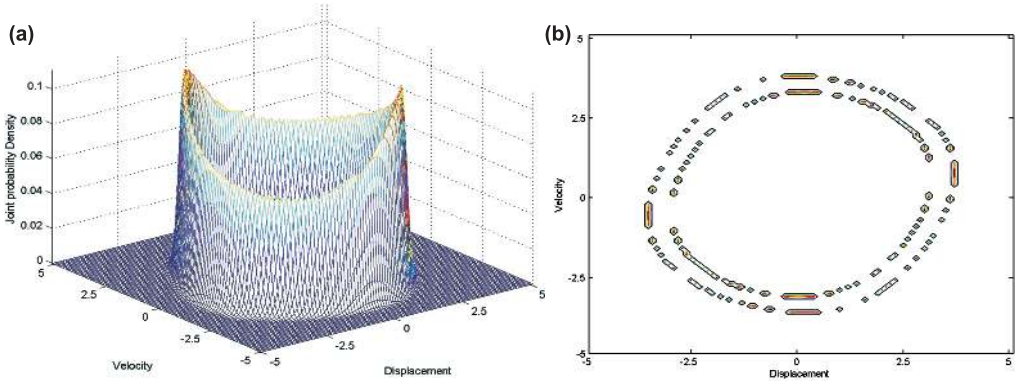

Figure 3. **(a)** Joint PDF. **(b)** Contour plot.

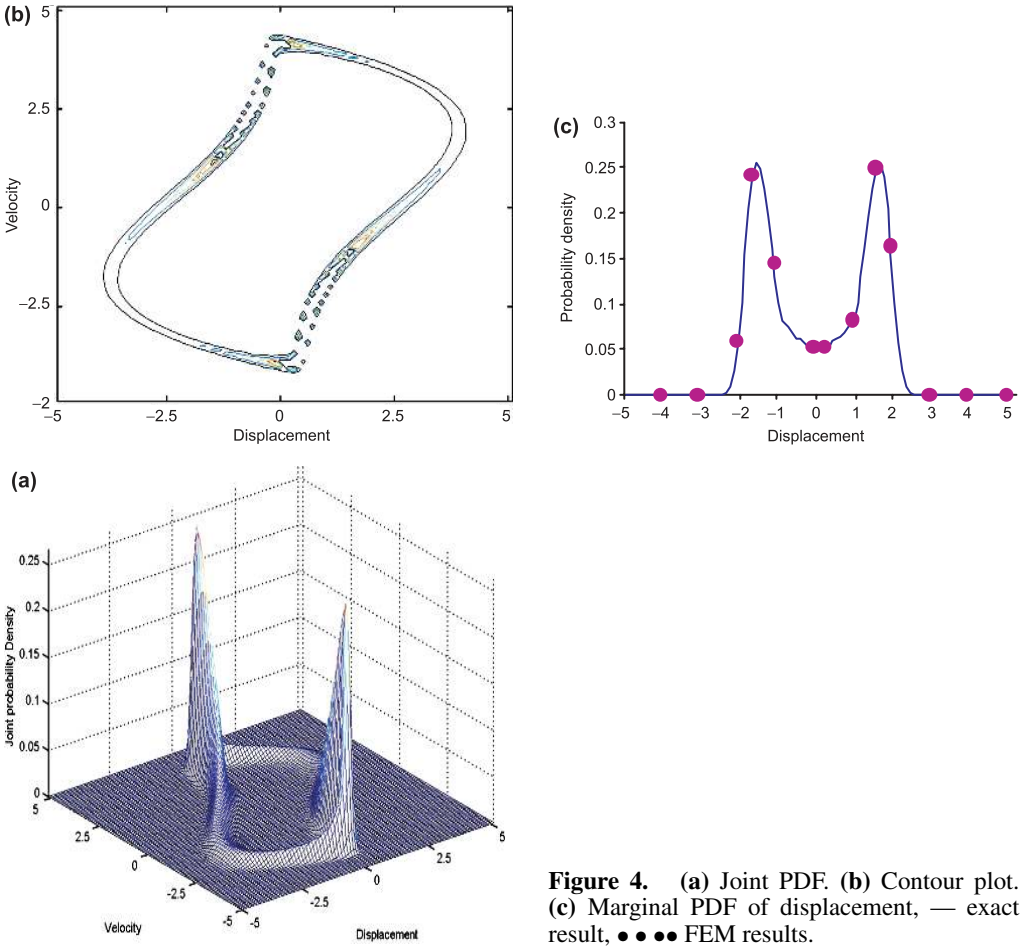

Figure 4. **(a)** Joint PDF. **(b)** Contour plot. **(c)** Marginal PDF of displacement, — exact result, • • •• FEM results.

5. Two-dimensional transient solution

As a second example, a hardening Duffing oscillator subjected to external and parametric white noise in the following form,

$$\ddot{X} + 2\xi\dot{X} + [W_1(t) - 1]X + \gamma X^3 = W_2(t), \tag{21}$$

is considered, where ξ, γ are constants and $W_1(t)$, $W_2(t)$ are independent zero mean Gaussian white noise processes with

$$\begin{aligned} E[W_1(t)W_1(t+\tau)] &= 2D_{11}\delta(\tau), \\ E[W_2(t)W_2(t+\tau)] &= 2D_{22}\delta(\tau). \end{aligned} \tag{22}$$

The corresponding FP equation is given by

$$\frac{\partial p}{\partial t} = \frac{\partial[(2\xi X_2 - X_1 + \gamma X_1^3)p]}{\partial X_2} - X_2\frac{\partial p}{\partial X_1} + (D_{11}X_1^2 + D_{22})\frac{\partial^2 p}{\partial X_2^2}, \tag{23}$$

where $X_1 = X$ and $X_2 = \dot{X}$.

The values of the parameters chosen are $\xi = 0{\cdot}2$, $\gamma = 0{\cdot}1$, $D_{11} = 0{\cdot}08$, $D_{22} = 0{\cdot}4$ with a bivariate Gaussian initial distribution with zero mean and variance of 0·5 in both dimensions. This system is particularly interesting since it has a bimodal stationary density function for small multiplicative excitation and is thus non–Gaussian. The grid size is again chosen as $[-5, 5] \times [-5, 5]$, which is divided into 100 elements per direction. The time step Δt of $\pi\pi/1000$ proves sufficient for good accuracy and a final time 10π is observed long enough for convergence to stationary conditions. For the case with no parametric excitation ($D_{11} = 0$) the joint PDF of this system is given in figure 5 at several instants of time, while figure 6. Presents marginal PDF of displacement and velocity at steady state. In figure 6, the exact solution is given by the full line and the FE solutions are given by this symbol •••. The solution for the stationary PDF in this case is given by Caughey (1971) and Caughey & Dienes (1962)

$$p(\boldsymbol{X}) = C \exp\left[\frac{X_1^2}{2} - \frac{X_2^2}{2} - \frac{\gamma X_1^4}{4}\right], \tag{24}$$

where C is the normalization constant. The accuracy of these finite element solutions is satisfactory, especially near the origin. The solution in the "tail" is less accurate than near the peaks.

Figure 7 gives the stationary joint PDF with small level of parametric excitation $D_{11} = 0{\cdot}08$ for $t = 31{\cdot}42$ s. In both the presence and absence of parametric excitation, the joint PDFs are bimodal. In the absence of parametric excitation the peaks are well separated, while in its presence the peaks merge.

6. Solution by the finite difference method

The FE solution of the FP equation is very accurate near the origin. However, the accuracy of the solutions near the tail regions is of the order of 10^{-4}, while it may be necessary that the probabilities have to be determined to an accuracy of order of 10^{-8} or higher for reliability studies. In the interest of improving the accuracy of the computational solution of the FP equation, particularly in the tails of the response distribution, as well as to simplify the methodology to some extent, higher order finite difference approximations have been developed by Wojtkiewicz *et al* (1994) for two-dimensional systems.

In this paper, higher order discretization schemes using finite difference methods are proposed to solve the FP equation up to the four dimension with a view to improve the accuracy of the probabilities in the tail region. The results reported here demonstrate that certain higher order schemes are capable of producing highly accurate solutions of the FP equations in the tail region of probability. This scheme involves the manipulation of Taylor's expansion of the density function about uniformly distributed nodal points in a n-dimensional mesh. The higher order scheme gives more accurate solution on a given mesh, allows for use of fewer mesh points and row population of the coefficient matrix is linear in the dimension of problem rather than exponential which leads to saving in memory and improvement of efficiency for a given mesh.

6.1 *Implementation of finite difference method for spatial discretization*

Through use of the Taylor expansion of the PDF about a selected point on a uniform mesh as displayed in figure 8, we can derive finite difference stencils of varying orders of accuracy.

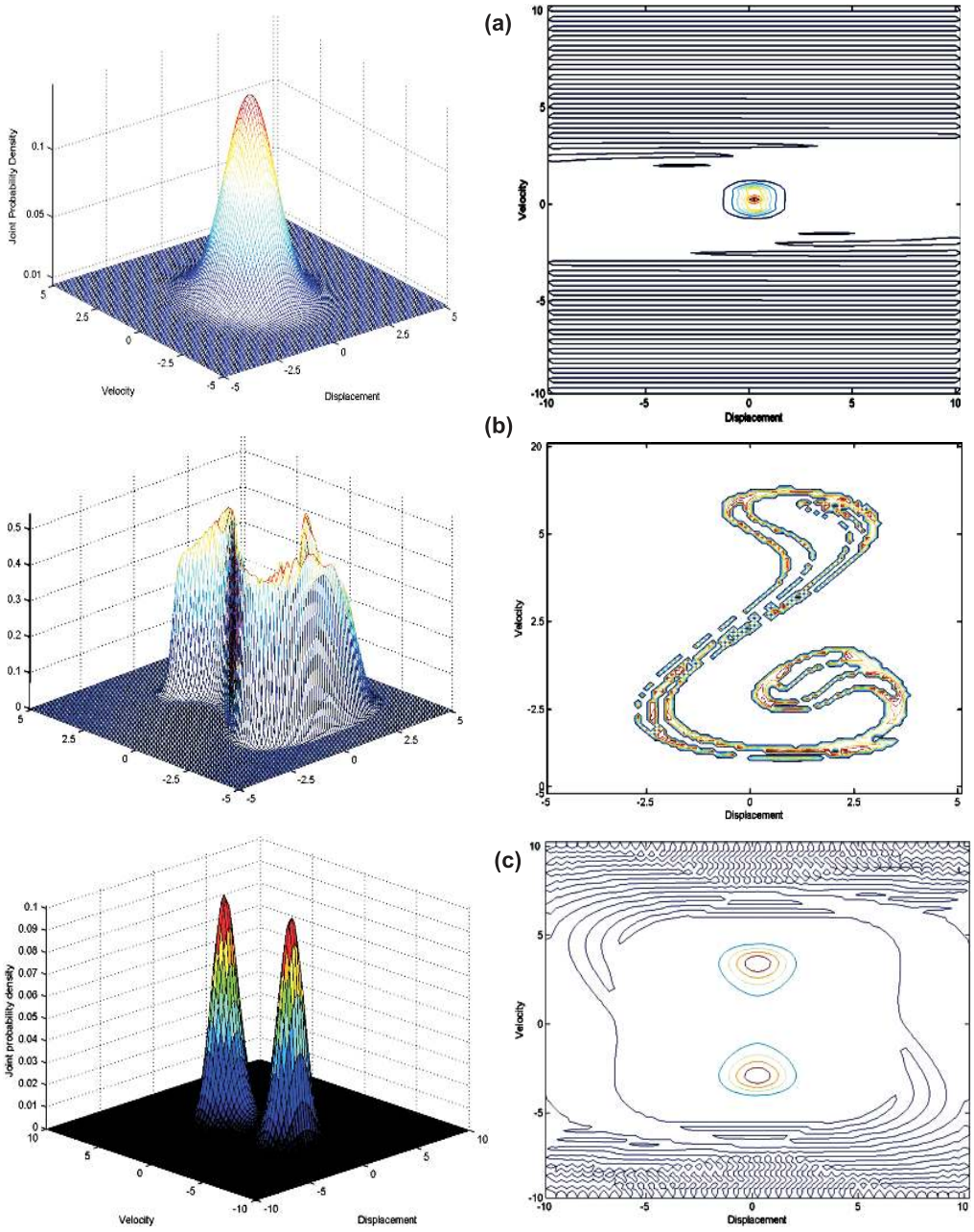

Figure 5. Snapshots of the joint PDF and contour plots of Duffing oscillator without parametric excitation ($D_{11} = 0$). $t = 1{\cdot}257$ s **(a)**, $3{\cdot}141$ s **(b)** and $30{\cdot}47$ s **(c)**.

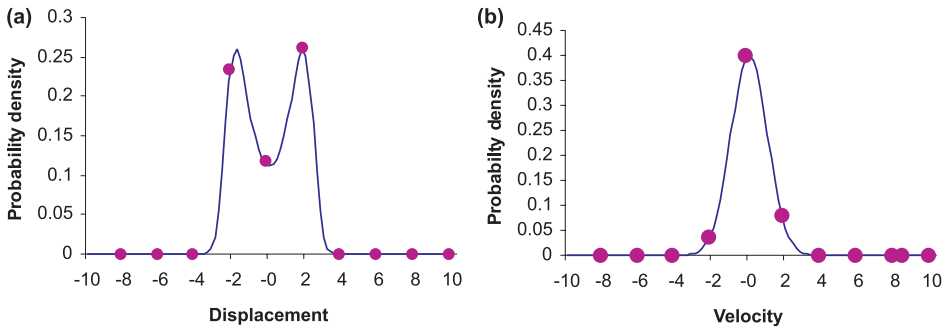

Figure 6. Marginal PDF of displacement **(a)**, and of velocity **(b)** of Duffing oscillator without parametric excitation ($D_{11} = 0$) at steady state, — exact result, • • •• FEM results.

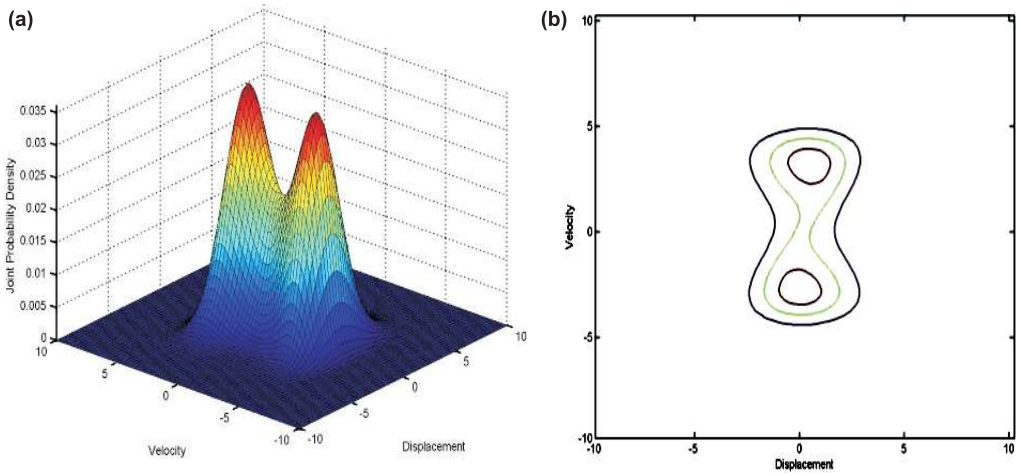

Figure 7. Stationary joint PDF and contour plots of Duffing oscillator with parametric excitation ($D_{11} = 0{\cdot}08$).

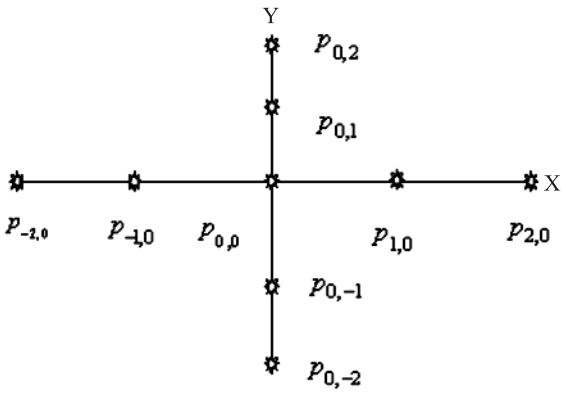

Figure 8. Finite difference discretization scheme for two-dimensional system.

Let $p_{i,j}$ denote the PDF at a discrete location relative to a candidate point as shown in figure 8 and given by

$$p_{i,j} = p(X + i\Delta X, Y + j\Delta Y). \tag{25}$$

The PDF $p_{1,0} = p(X + \Delta X, Y)$ and $p_{-1,0} = p(X - \Delta X, Y)$. These can be expressed in a Taylor series as

$$p_{1,0} = p_{0,0} + p'^{\Delta}_{0,0}X + \tfrac{1}{2}p''_{0,0}(\Delta X)^2 + 0(\Delta X^3), \tag{26}$$

$$p_{-1,0} = p_{0,0} - p'^{\Delta}_{0,0}X + \tfrac{1}{2}p''_{0,0}(\Delta X)^2 + 0(\Delta X^3). \tag{27}$$

Solving for the derivative terms at the candidate point gives

$$p'_{0,0} = \frac{\partial p(X,Y)}{\partial X} = \frac{p_{1,0} - p_{-1,0}}{2\Delta X} + 0(\Delta X^3), \tag{28}$$

$$p''_{0,0} = \frac{\partial^2 p(X,Y)}{\partial X^2} = \frac{p_{1,0} - 2p_{0,0} + p_{-1,0}}{(\Delta X)^2} + 0(\Delta X^3). \tag{29}$$

By using higher order Taylor series expansions and more of the neighbouring nodal points, higher order accuracy schemes can be derived. Second-, fourth-, sixth-, eight- and tenth-order schemes have been investigated; the tenth-order stencil, for example is given by (Wojtkiewicz *et al* 1994),

$$\frac{\partial p_{i,j}}{\partial X} = \frac{2100\alpha_1^X - 600\alpha_2^X + 150\alpha_3^X - 25\alpha_4^X + 2\alpha_5^X}{2520\Delta X},$$

where $\alpha_k^X = p_{k,0} - p_{-k,0}$,

$$\frac{\partial p_{i,j}}{\partial Y} = \frac{2100\alpha_1^Y - 600\alpha_2^Y + 150\alpha_3^Y - 25\alpha_4^Y + 2\alpha_5^Y}{2520\Delta Y},$$

where $\alpha_k^Y = p_{0,k} - p_{0,-k}$, and

$$\frac{\partial^2 p_{i,j}}{\partial Y^2} = \frac{42000\sum_1 - 6000\sum_2 + 1000\sum_3 - 125\sum_4 + 8\sum_5 - 36883\sum_0}{25200(\Delta Y)^2}, \tag{30}$$

where $\sum_k = p_{0,k} + p_{0,-k}$.

By substituting these into the FP equation, one equation in the nodal TPDF value may be formulated for each of the n nodes, resulting in a set of n discrete equations,

$$\dot{\boldsymbol{p}} + \boldsymbol{K}\boldsymbol{p} = \boldsymbol{0}. \tag{31}$$

For the stationary problem setting $\dot{\boldsymbol{p}} = \boldsymbol{0}$, we get the homogeneous equation $\boldsymbol{K}\boldsymbol{p} = \boldsymbol{0}$. The direct solution of the stationary problem is difficult as the system admits both a trivial solution $\boldsymbol{p} = \boldsymbol{0}$ and a nontrivial solution through enforcement of the normalization condition. It requires special handling, since iterative solutions tend to stagnate due to the indefiniteness in the coefficient matrix. An additional boundary condition can be applied making the degree of freedom at the origin constrained.

6.2 *Finite difference solution of duffing oscillator*

These higher order finite difference schemes are applied to the random vibration of a Duffing oscillator given by,

$$\ddot{X} + 2\xi\omega_n\dot{X} + \omega_n^2\gamma X + \omega_n^2\beta X^3 = W(t), \tag{32}$$

where $W(t)$ is the Gaussian white noise with a spectral density of $1/\pi$. Using the state space approach with $X_1 = X$ and $X_2 = \dot{X}$, we get

$$\begin{pmatrix} \dot{X}_1 \\ \dot{X}_2 \end{pmatrix} = \begin{bmatrix} X_2 \\ -2\omega_n\xi X_2 - \omega_n^2\gamma X_1 + \beta X_1^3 \end{bmatrix} + \begin{bmatrix} 0 & 0 \\ 0 & \pi^{-0\cdot5} \end{bmatrix} \begin{Bmatrix} 0 \\ W(t) \end{Bmatrix}, \tag{33}$$

with the corresponding stationary FP equation given by

$$-X_2\frac{\partial p}{\partial X_1} + \frac{\partial}{\partial X_2}(2\xi X_2 + \gamma X_1 + \beta X_1^3)p + \frac{\partial^2 p}{\partial X_2^2} = 0. \tag{34}$$

Equation (37) has an exact analytical solution given by Lin (Crandall 1963),

$$p(X_1, X_2) = C\exp\left\{-2\xi\omega_n\left(0\cdot5X_2^2 + \frac{1}{2}\omega_n^2X_1^2\gamma + \frac{1}{4}\omega_n^2\beta X_1^4\right)\right\}, \tag{35}$$

where C is chosen to satisfy the normalization condition. For the case $\omega_n = 1, \gamma = 1, \xi = 0\cdot5$ and $\beta = 0\cdot1$. The various order finite difference schemes are used to compute the marginal PDF of the response. The results obtained are compared with exact analytical solutions and with FEM results in table 1. The stationary PDF with the maximum absolute nodal error in the joint PDF and the marginal PDFs are given in table 2.

It is observed that the error levels decrease with increasing stencil order. The relative error in tail probabilities is less compared to that near the origin. It is also seen that higher order finite-difference schemes produce accurate solutions even in the tail portions. The second-order finite difference scheme gives a solution which is as accurate as the FEM solution. The tenth-order finite difference scheme gives a very low error level of 0·032% at a probability value of 10^{-8}.

Table 1. Probability density functions of response X^1 for a Duffing oscillator..

Response	FEM	Second-order finite diff.	Tenth-order finite diff.	Exact result [9]
0·0000	0·4762	0·4764	0·4760	0·4757
0·1500	0·4709	0·4708	0·4705	0·4703
0·3000	0·4550	0·4551	0·4545	0·4543
0·4500	0·4285	0·4286	0·4278	0·4277
0·6000	0·3919	0·3918	0·3911	0·3910
0·7500	0·3462	0·3460	0·3453	0·3452
0·9000	0·2932	0·2930	0·2924	0·2923
1·0500	0·2361	0·2360	0·2356	0·2355
1·2000	0·1789	0·1789	0·1788	0·1787
1·3500	0·1259	0·1261	0·1262	0·1263
1·5000	0·0811	0·0818	0·0820	0·0820
1·6500	0·0471	0·0481	0·0483	0·0483
1·8000	0·0242	0·0253	0·0254	0·0254

Table 2. Finite difference approximation error in joint PDF and marginal PDF of Duffing oscillator.

Method	Maximum absolute error in JPDF	Max. absolute error in x_1 marginal density	Max. absolute error in x_2 marginal density
Second-order finite difference	$1{\cdot}541 \times 10^{-3}$	$2{\cdot}864 \times 10^{-3}$	$2{\cdot}434 \times 10^{-3}$
Fourth-order finite difference	$3{\cdot}452 \times 10^{-5}$	$7{\cdot}887 \times 10^{-5}$	$2{\cdot}157 \times 10^{-5}$
Sixth-order finite difference	$2{\cdot}618 \times 10^{-6}$	$6{\cdot}681 \times 10^{-6}$	$4{\cdot}444 \times 10^{-7}$
Eight-order finite difference	$3{\cdot}378 \times 10^{-7}$	$8{\cdot}428 \times 10^{-7}$	$1{\cdot}424 \times 10^{-8}$
Tenth-order finite difference	$5{\cdot}516 \times 10^{-8}$	$1{\cdot}127 \times 10^{-8}$	$8{\cdot}498 \times 10^{-10}$
Finite element	$3{\cdot}602 \times 10^{-4}$	$8{\cdot}751 \times 10^{-4}$	$3{\cdot}551 \times 10^{-4}$

7. Scheme for four-dimensional problems

The FP equation has been numerically solved for systems with two and three states using both FEM and finite difference techniques. The extension of these solution algorithms to systems with more than three states is conceptually straightforward, but the task of calculating the joint probability density function of the state space Markov Vector process solving the nonlinear stochastic differential equation is a formidable problem. So far only a few solutions have been reported for four-dimensional problems. However, the accuracy of the obtained numerical solution in the tail regions of the PDFs are somewhat uncertain. Several issues are involved in designing an effective solution algorithm for such problems. These problems can be broadly categorized as:

i) Spatial and temporal discretization of the FP equation.
ii) Large size of system equations.

A system of coupled linear oscillators constituting a four-dimensional linear system is taken as an example. This system provides a benchmark to verify the accuracy of the algorithm. For transformation of the partial differential equation to a set of first-order differential equations a higher order discretization scheme using finite difference method has been applied. The scheme involves the manipulation of the Taylor series expansion of the PDF about uniformly distributed nodal point in a $n = 4$ dimensional mesh as shown in figure 9.

Figure 9 shows the mesh points for the discretization scheme for the finite difference method for a four-dimensional phase space on a computational mesh of 35^4 nodes, that is, 35 nodes per dimension of extent.

Let $p_{i,j,k,l}$ denote the PDF at a discrete location relative to a candidate point as shown in figure 9 and given by,

$$p_{i,j,k,l} = p(x + i\Delta x, y + j\Delta y, z + k\Delta z, w + l\Delta w). \tag{36}$$

The PDF values are $p_{1,0,0,0} = p(x + \Delta x, y, z, w)$ and $p_{-1,0,0,0} = p(x - \Delta x, y, z, w)$. These can be expressed in a Taylor series as,

$$p_{1,0,0,0} = p_{0,0,0,0} + p'_{0,0,0,0}\Delta X + \frac{1}{2}p''_{0,0,0,0}(\Delta X)^2 + O(\Delta X^3), \tag{37}$$

$$p_{-1,0,0,0} = p_{0,0,0,0} - p'_{0,0,0,0}\Delta X + \frac{1}{2}p''_{0,0,0,0}(\Delta X)^2 + O(\Delta X^3). \tag{38}$$

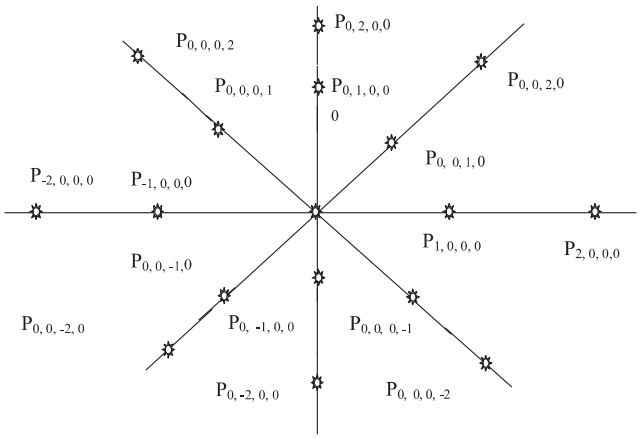

Figure 9. Finite difference scheme for spatial discretization for a four-dimensional system.

Solving for the derivative terms at the candidate point gives

$$p'_{0,0,0,0} = \frac{\partial p(X, Y, Z, W)}{\partial X}$$

$$= \frac{p_{1,0,0,0} - p_{-1,0,0,0}}{2\Delta X} + O(\Delta X^3), \tag{39}$$

$$p''_{0,0,0,0} = \frac{\partial^2 p(X, Y, Z, W)}{\partial X^2}$$

$$= \frac{p_{1,0,0,0} - 2p_{0,0,0,0} + p_{-1,0,0,0}}{\Delta X^2} + O(\Delta X^3). \tag{40}$$

We can derive finite difference stencils of varying order of accuracy by taking more neighbouring nodal points. By substituting these into the FP equation, one equation in the nodal TPDF may be formulated for each of the n-nodes, resulting in a set of n-discrete finite difference equation.

We consider the 2-degree-of-freedom system shown in figure 10 as an example to illustrate the method.

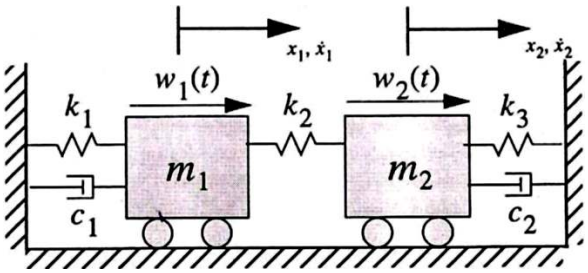

Figure 10. Four-dimensional linear system.

The equations of motion of the system in state space form is given by

$$\dot{\mathbf{X}} = \begin{bmatrix} 0 & 1 & 0 & 0 \\ -(k_1+k_2) & -c_1 & k_2 & 0 \\ 0 & 0 & 0 & 1 \\ k_2 & 0 & -(k_2+k_3) & -c_2 \end{bmatrix} \mathbf{X} + \begin{bmatrix} 0 & 0 \\ 0 & \sqrt{2D_1} \\ 0 & 0 \\ 0 & \sqrt{2D_1} \end{bmatrix} W(t), \tag{41}$$

where $W(t)$ is a Gaussian vector white noise process with

$$E[\mathbf{W}(t)] = 0,$$

$$E[\mathbf{W}(t_1)\mathbf{W}(t_2)] =: \begin{bmatrix} 2D_1 & 0 \\ 0 & 2D_2 \end{bmatrix} \delta(\tau),$$

$$\text{with} \quad \tau = t_2 - t_1. \tag{42}$$

The FP equation for this system is given by

$$\begin{aligned} \frac{\partial p}{\partial t} = {} & D_1 \frac{\partial^2 p}{\partial x_2^2} + D_2 \frac{\partial^2 p}{\partial x_4^2} - x_2 \frac{\partial}{\partial x_1}(p) - x_4 \frac{\partial}{\partial x_3}(p) + (k_1+k_2) x_1 \frac{\partial}{\partial x_2}(p) \\ & + c_1 x_2 \frac{\partial}{\partial x_2}(p) - k_2 x_3 \frac{\partial}{\partial x_2}(p) - k_2 x_1 \frac{\partial}{\partial x_4}(p) + (k_2+k_3) x_3 \frac{\partial}{\partial x_4}(p) \\ & + c_2 x_2 \frac{\partial}{\partial x_4}(p) + (c_1+c_2) p. \end{aligned} \tag{43}$$

For the system parameters $k_1 = k_2 = k_3 = 1, c_1 = c_2 = 0{\cdot}3$ and $D_1 = D_2 = 0{\cdot}3$ the problem is discretized using higher order finite difference scheme on a computational mesh of 35^4 nodes with range of $[-4, 4] \times [-4, 4] \times [-4, 4] \times [-4, 4]$. The initial conditions assumed are zero means for all the states and a four-dimensional Gaussian distribution with variance of $\sigma_i^2 = 0{\cdot}5$. A time step of $0{\cdot}005$ was used in the numerical integration.

The probability density function obtained by the finite difference scheme by taking a section corresponding to $t = 40{\cdot}5$ s for all the four states is denoted in figure 11 by the symbol • along with the closed form solution which is shown by the continuous line. The figure shows very good agreement between the two results.

8. Conclusions

In this paper the stationary and transient PDF of nonlinear dynamical oscillators subjected to random excitation have been obtained by FEM and high-order finite difference methods by the solution of the FP equations. Higher order finite difference methods are very accurate in predicting the joint PDFs for two-dimensional problems even at the low probability levels ($\leq 10^{-6}$) in the tail regions of the PDF. Stationary solutions obtained by these spatial discretization methods to four-dimensional linear problems are also very accurate.

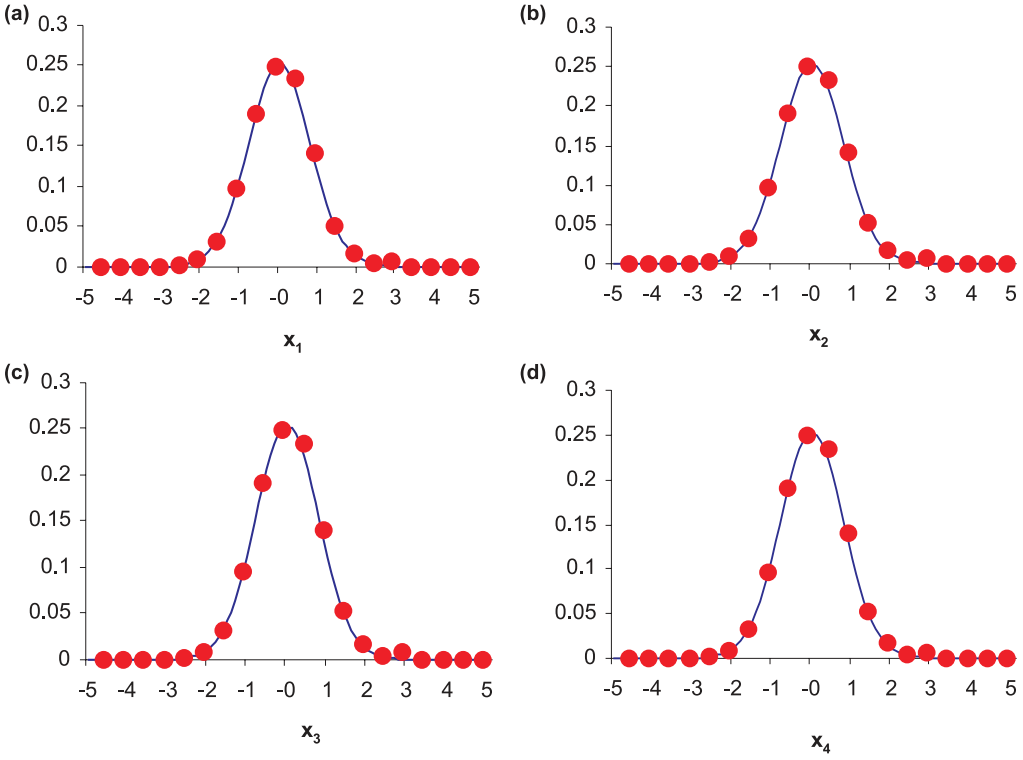

Figure 11. Cross sections of the density function of the linear system through the origin at $t = 40{\cdot}5$ s; — exact, • • •• finite difference method results.

References

Caughey T K 1971 Nonlinear theory of random vibrations. In *Advances in applied mechanics* (ed.) C-S Yih (New York: Academic Press) 11: 209–253

Caughey T K, Dienes J K 1962 The behaviour of linear systems with white noise input. *J. Math. Phys.* 32: 2476–2479

Crandall S H 1963 Perturbation techniques for random vibration of nonlinear systems. *J. Acoust. Soc. Am.* 35: 1700–1705

Johnson E A, Wojtkiewicz S F, Bergman L A, Spencer B F Jr 1997a Observations with regard to massively parallel computation for Monte Carlo simulation of stochastic dynamical systems. *Int. J. Nonlinear Mech.* 32(4): 721–734

Johnson E A, Wojtkiewicz S F, Spencer B F Jr, Bergman L A 1997b Finite element and finite difference solutions to the transient Fokker–Planck equation. DESY–97-161: 290–306

Khasminskii R Z 1996 A limit theorem for the solution of differential equations with random right-hand sides. *Theor. Probab. Appl.* 11: 390–405

Kunert A 1991 Efficient numerical solution of multi-dimensional Fokker–Planck equations with chaotic and nonlinear random vibration. In *Vibration analysis – Analytical and computational* (eds.) T C Huang *et al* DE-37: 57–60

Langley R S 1985 A finite element method for the statistics of nonlinear random vibration. *J. Sound Vibr.* 101: 41–54

Langtangeh H P 1991 A general numerical solution method for Fokker–Planck equations with applications to structural reliability. *Probab. Eng. Mech.* 6: 33–48

Lin Y K 1967 *Probabilistic theory of structural dynamics* (New York: McGraw Hill)

Naess A, Johnson J M 1992 Response statistics of nonlinear dynamics systems by path integration. In *Proc. IUTAM Symp. on Nonlinear Stochastic Mechanics*, (eds) N Bellomo, F Casciatti (Berlin: Springer-Verlag) pp 401–414

Risken H 1989 *The Fokker–Planck equation: Methods of solution and applications* (New York: Springer-Verlag)

Roberts J B, Spanos P D 1990 *Random vibration and statistical linearization* (Wiley: New York)

Schueller G I, Pradlwarter H J, Pandey M D 1993 Methods for reliability assessment of nonlinear system under stochastic dynamic loading – A review. In *Structural dynamics: Proc. Second European Conf. on Structural Dynamics: EURODYN'93* (eds) T Moan *et al* 1993 (Rotterdam: Balkema) pp 751–759

Soong T 1994 *The Fokker–Planck equation for stochastic dynamical system and its explicit steady state solution* (Singapore: World Scientific)

Spencer Jr B F, Bergman L A 1993 On the numerical solution of the Fokker equations for nonlinear stochastic systems. *Nonlinear Dynamics* 4: 357–372

Sun J Q, Hsu C S 1988 First-passage time probability of nonlinear stochastic systems by generalized cell mapping method. *J. Sound Vibr.* 124: 233–248

Sun J-Q, Hsu C S 1990 The generalized cell mapping method in nonlinear random vibration based upon short-time Gaussian approximation. *ASME J. Appl. Mech.* 57: 1018–1025

Wang M C, Uhlenbeck G 1945 On the theory of Brownian motion II. *Rev. Modern Phys.* 17: 323–342 (reprinted 1954 in *Selected papers on noise and stochastic processes* (ed.) N Wax (New York: Dover)

Wen Y K 1976 Method for random vibration of hysteretic systems. *ASCE J. Engineering Mech.* 102(EM2): 249–263

Wojtkiewicz S F, Bergman L A, Spencer B F Jr 1994a Robust numerical solution of the Fokker–Planck–Kolmogorov equation for two-dimensional stochastic dynamical systems. Technical Report AAE 94-08, Department of Aeronautical and Astronautical Engineering, University of Illinois at Urbana-Champaign, Urbana-Champaign, IL

Wojtkiewicz S F, Bergman L A, Spencer B F Jr 1994b High fidelity numerical solutions of the Fokker–Planck equation. *Proc. ICOSSAR'97, the 7th Int. Conf. on Structural Safety and Reliability*, Kyoto, Japan

Wojtkiewicz S F, Spencer B F Jr, Bergman L A 1996 On the cumulant-neglect closure method in stochastic dynamics. *Int. J. Nonlinear Mech.* 31: 657–684

Wong E, Zakai M 1965 On the relation between ordinary and stochastic differential equation. *Int. J. Eng. Sci.* 31965: 213–229

Wu W F, Lin Y K 1984 Cumulant-neglect closure for nonlinear oscillators under parametric and external excitations. *Int. J. Nonlinear Mech.* 19: 349–362